JOURNAL OF MATERIALS SCIENCE 35 (2000) 6251–6258

Corrosion of alumina ceramics in acidic aqueous solutions at high temperatures and pressures

M. SCHACHT*, N. BOUKIS*, E. DINJUS
Forschungszentrum Karlsruhe, Institut für Technische Chemie, 76021 Karlsruhe, Germany
E-mail: Michael.schacht@hrt.fzk.de

Alumina is resistant against corrosive aqueous solutions and could be used as a reactor material in the Supercritical Water Oxidation (SCWO) process. For this reason, the corrosion resistance of alumina and zirconia toughened alumina (ZTA) ceramics was investigated in aqueous solutions containing 0.1 mol/kg H_2SO_4, H_3PO_4 or HCl at $T = 240^\circ$C–500°C at $p = 27$ MPa. In sulfuric acid, the solubility of alumina and its corrosion products was high at temperatures of 240°C–290°C. The corrosion rate was still high at higher temperatures (340°C–500°C), but the corrosion products were less soluble and formed a non-protecting scale on the samples. Phosphoric acid was less corrosive due to the formation of berlinite ($AlPO_4$) on the surface of the specimens. In hydrochloric acid, the dissolution of the alumina grains was the predominant corrosion phenomenon at temperatures of 240°C–290°C. At higher temperatures, intergranular corrosion was observed, but a dissolution of the grains did not occur. © *2000 Kluwer Academic Publishers*

1. Introduction

Alumina is known to be corrosion resistant in corrosive aqueous solutions at elevated temperatures [1–6]. As a consequence, alumina could be used as a reactor material in the Supercritical Water Oxidation (SCWO) process, although its machining is difficult. In the SCWO process, hazardous or toxic aqueous wastes containing organic contaminants are rapidly and quantitatively oxidized to harmless compounds at temperatures of about 500°C and pressures of 24 to 30 MPa [7]. At these conditions, water exhibits properties similar to those of a dense gas, including complete miscibility with nonpolar organic substances and gases like oxygen and nitrogen. In a single-phase reaction medium containing water, organics and oxidizer (e.g. oxygen or air), the organic waste is rapidly oxidized.

The major problem for the safe operation of a SCWO plant is the corrosion of the reactor material when wastes containing heteroatoms like Cl, S or P are oxidized. Stainless steels [8], nickel-base alloys [8–11] and most of the ceramic materials [12] are attacked severely by the formed acids and reactors made of these materials fail after few hours. An improvement in corrosion resistance could be achieved by the fabrication of reactors with an inner surface consisting of nonporous alumina ceramics. However, no systematic experiments on the corrosion resistance of alumina ceramics in acid containing SCWO environments were performed. The published work on the corrosion of alumina in aqueous solutions [1–6] is limited to experimental temperatures of $<300^\circ$C.

In high temperature water (300°C, 8.6 MPa), alumina ceramics with 99% [1] and 99.3% Al_2O_3 [2] are attacked by dissolution of a Si-, Ca- and Na-containing grain boundary phase. No intercrystalline corrosion was found on high-purity alumina (>99.9% Al_2O_3) [1]. Dawihl and Klingler [3] found that an alumina ceramic with 99.9% Al_2O_3 is only slightly attacked in boiling concentrated hydrochloric acid. On the other hand, concentrated sulfuric acid is very corrosive on 99.9% Al_2O_3 at temperatures above 100°C. Genthe and Hauser [4–6] investigated the corrosion resistance of alumina ceramics, doped with MgO, Y_2O_3, Cr_2O_3, ZrO_2, BaO, and SiO_2, respectively, at temperatures up to 180°C in concentrated HCl, H_2SO_4, and H_3PO_4, respectively. The authors found that the corrosive effect of the acids on alumina decreases in the order $H_3PO_4 > HCl > H_2SO_4$.

All investigations showed that the corrosion resistance of alumina ceramics is influenced by the purity of the material due to a segregation of impurities to the grain boundaries during the sintering process. Detrimental is the presence of SiO_2 in concentrations above some 1000 ppm, which causes the formation of a silicate-rich glassy phase on the grain boundaries. This phase is attacked easily by mineral acids. After dissolution of the grain boundary phase, the grains are completely exposed to the corrosive medium and are finally washed out. Furthermore, the porosity and the microstructure of the ceramic material are important for the corrosion resistance. Al_2O_3 ceramics with closed porosity and large grain sizes are more resistant to corrosive attack.

To evaluate, if Al_2O_3 is suitable as reactor material for the SCWO process, a detailed investigation on the corrosion resistance of alumina ceramics with different

* Author to whom all correspondence should be addressed.

chemical compositions in acid containing aqueous solutions at temperatures between 240°C and 500°C and a pressure of 27 MPa is performed.

2. Experimental procedure

Samples of 99.99% alumina, prepared from the Taimei DAR powder (TAI), a commercially available monolithic alumina (99.7% Al_2O_3, ALC) and a zirconia toughened alumina (ZTA) were used in this study. The ceramic discs were cut into bars (23 mm × 9 mm × 4 mm) and polished to a mirror-like surface using 1 μm diamond paste.

The samples were placed in a corrosion resistant tube reactor [13] and subjected to aqueous 0.1 mol/kg HCl, H_2SO_4, or H_3PO_4 for 50 hours. The experimental pressure was 27 MPa and the temperatures were 240°C, 290°C, 340°C, 390°C, and 500°C, respectively. Additionally, two experiments were performed at 420°C and 440°C using aqueous 0.1 mol/kg HCl as corrosive medium. ZTA was not investigated in H_2SO_4 at temperatures higher than 290°C.

After the corrosion experiments, the specimens were dried in a vacuum oven and weight loss was determined. The surface and cross sections of the corroded specimens were analysed with scanning electron microscopy (SEM, LEO Gemini 982) and energy-dispersive X-ray analysis (EDX, Oxford Link ISIS 300). Surface layers and the content of the monoclinic phase of ZrO_2 in ZTA were examined with powder X-ray diffraction analysis (XRD, Siemens D 5000, Cu $K_{\alpha 1,2}$-radiation).

For the determination of the chemical composition of the aluminas, 0.1–0.3 g of the different materials were pulverized in a ball mill with tungsten carbide lining and tungsten carbide grinding balls. The resulting powder was melted in a platinum crucible with an excess of $Li_2B_4O_7$. The melt was dissoved by a treatment with boiling semiconcentrated hydrochloric acid. The solution was diluted and analyzed with optical emission spectroscopy with inductively coupled plasma (ICP-OES, Varian Spectra 150).

3. Materials characterization

ALC, a typical commercial high performance Al_2O_3 ceramic, contains MgO as sintering aid and the usual impurities SiO_2, CaO, Fe_2O_3 and TiO_2. The particle size distribution is broad, and the grains have mostly an elongated shape.

Due to the dispersion of ZrO_2 particles in the Al_2O_3 matrix, the Al_2O_3 grains in ZTA are smaller and shaped more uniformly than those in ALC. The ZrO_2 grains are located in the form of irregular shaped particles along the boundaries of the alumina grains or on the junctions between three or four Al_2O_3 grains.

The microstructure of the high purity alumina TAI consists mostly of equiaxed grains. Pores are smaller and less frequent than in the commercial products ALC and ZTA. Tables I and II list the chemical compositions, the densities and average grain sizes of the different Al_2O_3 ceramics. The microstructures are shown in the Figs 1–3.

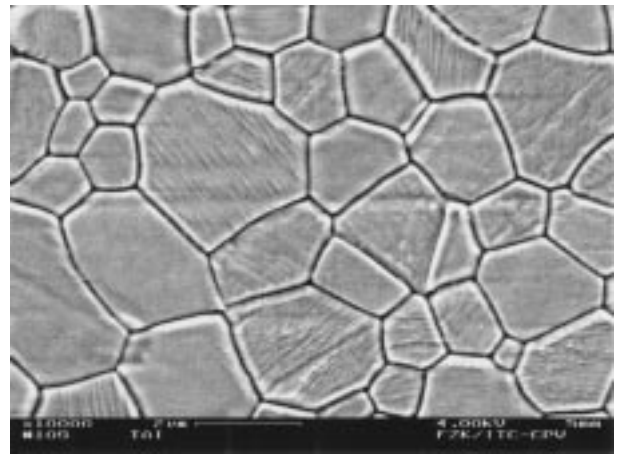

Figure 1 Microstructure of TAI.

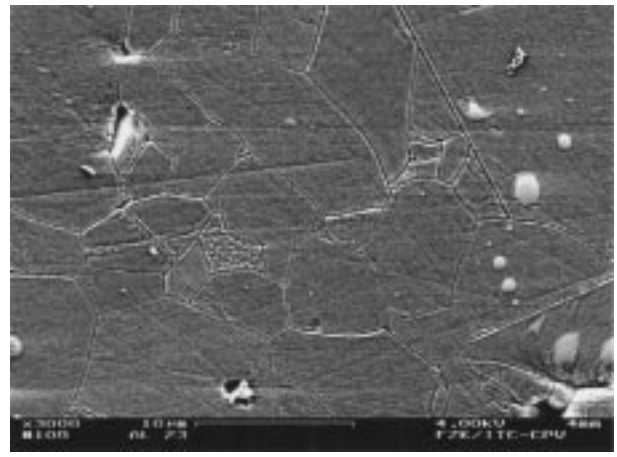

Figure 2 Microstructure of ALC.

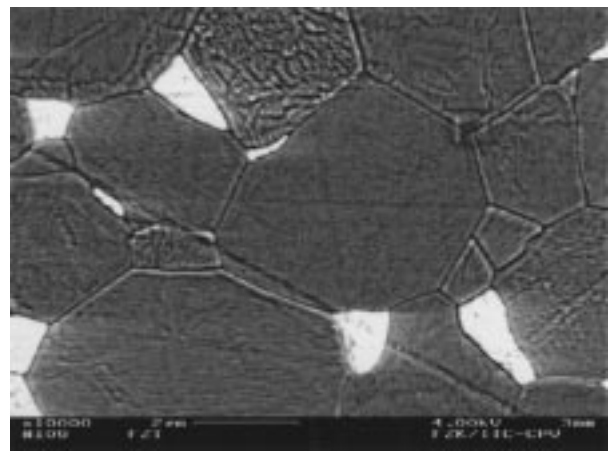

Figure 3 Microstructure of ZTA.

4. Results

4.1. Corrosion in hydrochloric acid

As is shown in the Figs 4 and 5, the influence of temperature on the corrosion resistance of the alumina ceramics is very strong. At temperatures of 240°C and 290°C, most grains were attacked by the formation of etching channels due to the dissolution of alumina (Fig. 4). A few very small alumina grains were removed from the surface of the ceramics. Fig. 5 shows that the maximum weight loss of the TAI and ALC specimens was found at an experimental temperature of

TABLE I Chemical composition of the materials

	ZrO_2 [wt%]	Y_2O_3 [wt%]	SiO_2 [ppm]	MgO [ppm]	Fe_2O_3 [ppm]	CaO [ppm]	TiO_2 [ppm]
TAI	—	—	17	2	10	2	—
Al23	—	—	430	2700	700	180	50
ZTA	9.23	0.74	810	500	12200	170	130

TABLE II Grain size and density of the materials

	Average grain size [μm]	Density [kg/m^3]
TAI	1.7	3920
Al23	13	3890
ZTA	5 ($A1_2O_3$), <2 (ZrO_2)	4070

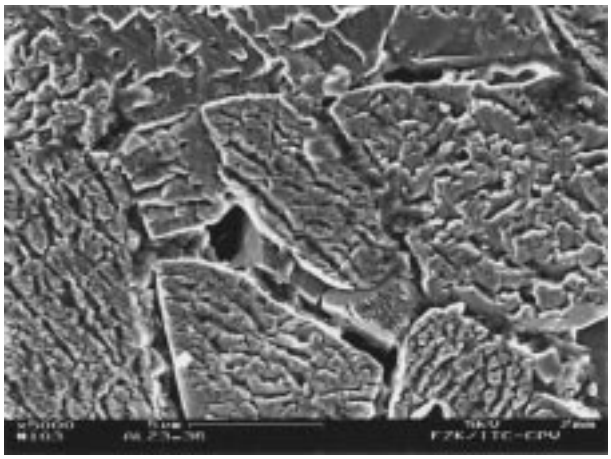

Figure 4 Etching channels on the surface of ALC (HCl, 50 h, 240°C, 27 MPa).

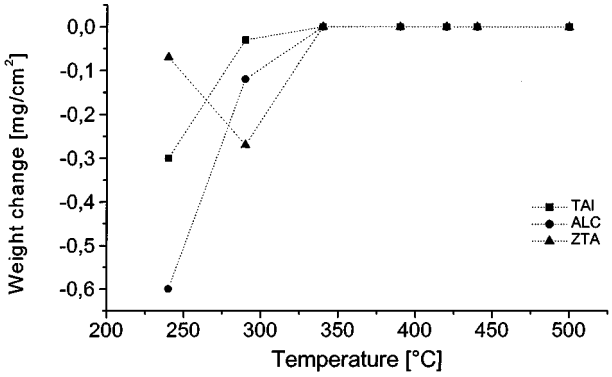

Figure 5 Weight change of the materials in HCl (50 h, 27 MPa).

240°C and fell with increasing temperature, while ZTA showed the highest weight loss at 290°C. At temperatures above 340°C, no weight change could be found anymore.

As shown in Fig. 6, the penetration depth of HCl in TAI is low at temperatures of 240°C–390°C, reaches a maximum at 420°C and drops with increasing temperature again. Compared with TAI, ALC is less resistant against intergranular corrosion in HCl. The penetration depth in ALC, represented in Fig. 4, is higher by a factor of 4–18 but shows a similar temperature dependency. It is low at 240°C and 290°C, increases strongly with increasing temperature, reaches a maximum at 420°C

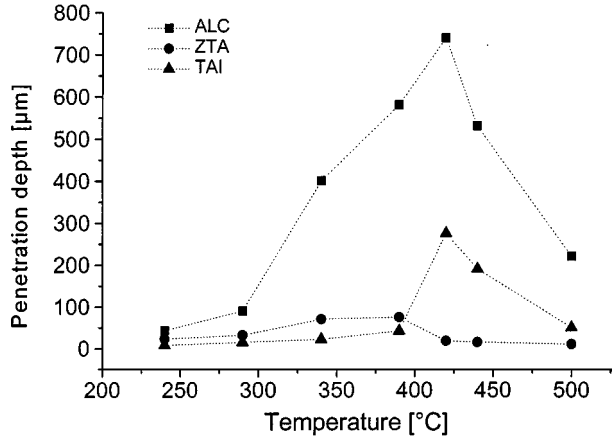

Figure 6 Penetration depth of 0.1 mol/kg HCl in ALC, TAI and ZTA.

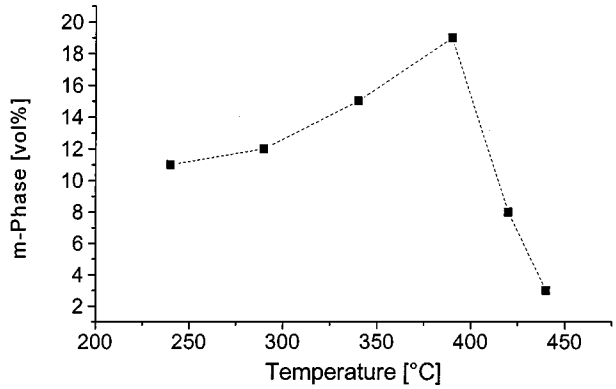

Figure 7 Content of m-ZrO_2 on the surface of ZTA (HCl, 50 h, 27 MPa).

and then drops to lower values with a further increase in temperature.

A comparison of the intensity of intergranular corrosion of ZTA and the high purity alumina TAI reveals (see Fig. 6) that the grain boundaries of ZTA are – despite the high impurity content of the ceramic – surprisingly corrosion resistant. This behaviour is extremely pronounced in the temperature range between 420°C and 500°C. The ZrO_2 particles on the grain boundaries are also susceptible to corrosive attack in HCl under these conditions due to a partial transformation of the cubic ZrO_2 into monoclinic ZrO_2. Fig. 7 shows that the content of monoclinic ZrO_2 increases with increasing the temperature from 240°C to 390°C and then decreases below 10 vol%.

4.2. Corrosion in sulfuric acid

Although alumina is attacked in H_2SO_4 in the temperature range between 240°C and 290°C by dissolution, the corrosion resistance of the alumina ceramics is stongly dependent on their chemical composition. High purity of the material (TAI) and the dispersion of ZrO_2 particles (ZTA) have a positive influence on the corrosion resicstance of alumina ceramics. Corrosion layers were not formed in this temperature range.

Etching channels have developed on grains on the initial surface of ALC and ZTA. In the case of ALC, most of these grains remained only loosely fixed on the surface due to the preferred dissolution of the grain

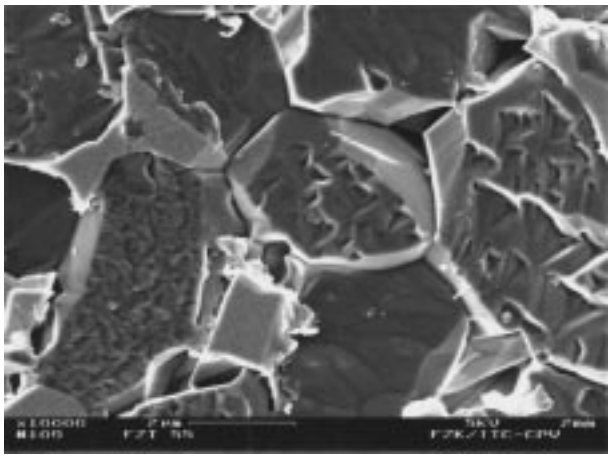

Figure 8 Surface of ZTA (H_2SO_4, 50 h, 240°C, 27 MPa).

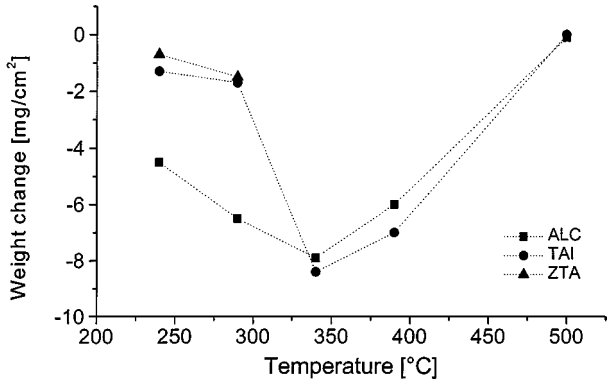

Figure 9 Weight change in H_2SO_4 after removing the corrosion products (50 h, 27 MPa).

boundaries and grain boundary neighbouring regions or were already washed out of the surface of the ceramic.

Despite the high impurity content of ZTA, the stability of its grain boundaries against H_2SO_4 is higher than the stability of ALC grain boundaries. Fig. 8 shows that no washing out of ZTA grains occured at a temperature of 240°C. This results in a considerable lower weight loss and lower penetration depth.

The ZrO_2 particles of ZTA are attacked only little. A small increase of the amount of m-ZrO_2 from 7 vol% (untreated sample) to 11 vol% or 17 vol% after the exposure in H_2SO_4 at 240°C or 290°C was determined.

In the temperature range of 340–390°C, porous, up to 20 μm thick corrosion layers were found on ALC and TAI. According to EDX measurements, all these layers have almost the same chemical composition: 12 ± 1 mol% sulfur, 13 ± 1 mol% aluminum and 75 ± 2 mol% oxygen. After removing the layers, TAI and ALC showed similar weight losses (Fig. 9). The penetration depths in the samples decreased with increasing the temperature from 340°C to 390°C (Fig. 9).

At a temperature of 500°C, only a very thin corrosion layer can be found on the exposed samples. A weight loss of less than 0.1 mg/cm^2 was measured. The penetration depth of sulfuric acid in ALC continues to decrease, while it increases strongly at TAI (Fig. 10). The corrosion of ZTA was not examined in the temperature range between 340°C and 500°C.

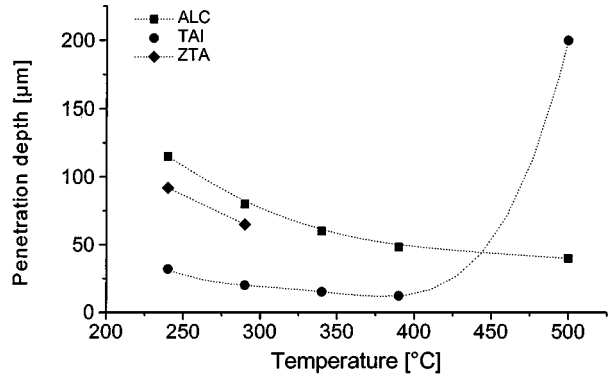

Figure 10 Penetration depth of 0.1 mol/kg H_2SO_4 in ALC, TAI and ZTA (50 h, 27 MPa).

4.3. Corrosion in phosphoric acid

In 0.1 mol/kg phosphoric acid, the alumina ceramics and ZTA were attacked in the temperature range between 240°C and 500°C by formation of berlinite ($AlPO_4$). The $AlPO_4$-scale on the samples was less than 2 μm thick. The penetration depths were small with 14–18 μm for TAI and ZTA or 24–30 μm for ALC and were not temperature-dependent. The weight loss, which was measured after removing the corrosion layer, was low with only 0.1–0.3 mg/cm^2. The ZrO_2 particles of ZTA were not attacked. The amount of monoclinic ZrO_2 on the surface of ZTA was unchanged compared with those of the untreated sample.

5. Discussion

The corrosion of alumina ceramics in aqueous solutions is determined by the solubility of alumina and the solubilities of the grain boundaries phases. Furthermore, the solubility of the corrosion products is of crucial importance for the corrosion resistance of the aluminas. An estimation of the chemical composition of the grain boundaries of the examined aluminas is made on the basis of literature data. The influence of the grain boundary composition, the corrosive agent and the temperature on the intergranular corrosion and the weight loss in aqueous solutions at 27 MPa and 240°C–500°C is discussed below.

5.1. Grain boundaries in polycrystalline alumina

For the evaluation of the influence of the grain boundaries on the corrosion resistance of the ceramic materials the chemical composition of the grain boundaries is important. Since no measurements of grain boundary compositions were performed in this study, literature data have to be taken into account. The distribution of the impurities is specified by the solubility of the cations in the alumina lattice. These solubilities are small due to the differences in the charge and ionic radius of Mg^{2+} (72 pm), Ti^{4+} (68 pm), Zr^{4+} (72 pm), Ca^{2+} (100 pm) Si^{4+} (42 pm) compared with the charge and ionic radius of Al^{3+} (53.5 pm) [14, 15]. Ca^{2+} possesses the smallest solubility.

If the solubility limit of the cations in Al_2O_3 is exceeded, they segregate to the grain boundaries of the ceramic materials. The enrichment of Ca^{2+} is very high with a factor of up to 4800, whereby certain grain boundaries are preferred [16–18]. If Mg^{2+} is present in the ceramic beside Ca^{2+}, then the enrichment of Ca^{2+} is smaller and its distribution is more homogeneous [18, 19]. The grain boundaries of alumina ceramics containing 2–10% of $CaSiO_3$ showed a strong enrichment of calcium, whereas both calcium and silicon are enriched in triple grain junctions [20].

Silicon [21–23], yttrium [24], zirconium [24–27] and titanium [21] also segregate to the grain boundaries of polycrystalline alumina. The enrichment of zirconium on the grain boundaries of ZTA was observed by Flacher *et al.* [28]. The behaviour of Mg^{2+} in alumina ceramics was still discussed controversely [29], as the enrichment of Mg^{2+} at free sapphire surfaces already was proven [30, 31]. Not until 1995 the segregation of Mg^{2+} to the grain boundaries of an alumina ceramic was found [19]. Later, this result was verified by other authors [24, 25]. It was found that the presence of magnesium in polycrystalline alumina suppresses the enrichment of silicon at the grain boundaries by the increase of the solubility in the alumina lattice [22].

Furthermore, the change of the binding state due to the enrichment of Mg^{2+} or Zr^{4+} at the grain boundaries of Mg- and Zr-doped aluminas was examined [25]. By means of electron energy loss spectroscopy (EELS) it was found that the bonding between cations and oxygen is weakened by Mg^{2+}, but strengthened by Zr^{4+}. If the solubility limit of Si^{4+}, Ca^{2+} or Mg^{2+} on the grain boundaries is exceeded, then an amorphous, glassy second phase is formed there. Since many eutectics exist in the CaO-SiO_2-Al_2O_3-system in the temperature range of 1200°C–1400°C, the formation of a Ca- and Si-rich grain boundary phase is preferred.

For the grain boundaries of the examined alumina ceramics the following is concluded: The material TAI contains only 8 ppm of Si, 7 ppm of Fe, 4 ppm of Na and 1 ppm of Mg and Ca. A segregation of Si, Na, Ca and Mg to the grain boundaries will take place, but the concentration at the grain boundaries is not sufficient for the formation of a grain boundary phase. The segregation of Fe is not examined in the literature. Since Fe^{3+} carries the same charge as Al^{3+} and is not substantially larger (ionic radius Fe^{3+} 64 pm, Al^{3+} 53.5 pm), only a small enrichment of Fe at the grain boundaries is expected. The commercially available ceramic ALC contains 1600 ppm of Mg, 480 ppm of Fe, 200 ppm of Si, 130 ppm of Ca and 30 ppm of Ti. Here, a grain boundary phase is certainly present. Since the doping with Mg increases the solubility of Si^{4+} in the alumina lattice, its formation is drastically limited. The transformation toughened material ZTA is very strongly contaminated with Fe (8450 ppm). Beside Fe, Mg (300 ppm), Si (370 ppm), Ca (120 ppm) and Ti (80 ppm) is found in the ceramic. Here, the formation of a Ca-, Si- and Al-enriched grain boundary phase and the enrichment of Zr at the grain boundaries is probable.

5.2. Intergranular corrosion

5.2.1. Influence of the grain boundaries and grain boundary phases

The enrichment of cations with charges and ionic radii different than that of Al^{3+} like Si^{4+}, Na^{+}, Ca^{2+} and Mg^{2+} on the grain boundaries causes a straining of the alumina lattice leading to a decrease of the binding energy [25] with increasing impurity content. This facilitates the attack of the corrosive solution at these places. Consequently, TAI, the alumina ceramic with the highest purity and the lowest amount of pores, has the most stable grain boundaries. A reason for the reported exceptions - HCl at temperatures higher than 420°C and H_2SO_4 at 500°C - could be a grain size effect, i.e. the higher number of grain boundaries in ceramics with a small grain size. This effect could gain importance at temperatures over approx. 400°C, where the grain boundary stability of the investigated alumina ceramics are similar due to a reduction of the solubility of the silicate-rich grain boundaries of the commercial-grade alumina ceramics ALC and ZTA in aqueous acidic solution solutions.

If the ceramic has a very high impurity content, a crystalline or amorphous grain boundary phase is formed and intergranular attack becomes stronger due to a high solubility of this phases in aqueous acidic solution solutions. For this reason, ALC is most susceptible to intergranular corrosion.

Despite its high impurity content, the material ZTA shows in all acids just as small intergranular corrosion as the high purity material TAI. This can only be explained with the increase of the stability of the grain boundaries by the ZrO_2-particles and the enrichment of Zr at the grain boundaries, as it was observed by Wakai *et al.* [26] and Yoshida *et al.* [27] in alumina ceramics doped with 1000 ppm of ZrO_2.

5.2.2. Influence of the temperature and the corrosive species

In HCl, the intergranular corrosion of the investigated alumina ceramics is small up to a temperature of 290°C. If the temperature is increased to 340°C, the penetration depth increases rapidly. The increase in temperature increases the rate of the dissolution of the grain boundaries and grain boundary phases and thus causes the increase of the intergranular corrosion.

It is expected that the solubility of the impurities on the grain boundaries in 0.1 mol/kg HCl decreases with increasing the temperature over 360°C, and is highest for the grain boundary phase in ALC. Since the intergranular corrosion of TAI and ALC is high up to 420°C, it is assumed that the dissolution of the grain boundaries and the diffusion of HCl along the grain boundaries remain high up to this temperature and drop to low values with a further increase in temperature. However, literature data to prove this assumption are not available.

In ZTA, the intensity of intergranular corrosion is influenced strongly by the stability of the Y-CSZ-particles on the grain boundaries, since they counteract the progressing of intergranular corrosion. Below 390°C, these particles are attacked by dissolution of yttria, and a

cubic to monoclinic phase transformation takes place, while they are stable at temperatures above 420°C. Thus, the intensity of intergranular corrosion increases up to a temperature of 390°C and decreases again at temperatures above 420°C.

In H_3PO_4, the intergranular corrosion is suppressed by the fast formation of an insoluble $AlPO_4$-layer, which protects the alumina ceramics against further attack. The penetration depths are small and not temperature-dependent. H_3PO_4 attacks the grain boundaries of alumina ceramics in the temperature range between 240°C and 500°C less than HCl or H_2SO_4.

In diluted, oxygen-containing H_2SO_4, the penetration depth of the corrosive solution in the materials becomes smaller with increasing temperature in the temperature range from 240°C to 390°C. At temperatures above 340°C, the diffusion of H_2SO_4 to the ceramic surface is hampered due to the formation of a porous Al-, S- and O-containing layer, but it is not prevented. Although this corrosion layer is by a factor of 10 thicker than the $AlPO_4$-layer formed in H_3PO_4, H_2SO_4 diffuses faster through this layer than H_3PO_4 through the $AlPO_4$-layer.

At 500°C, the penetration rate continues to slow down at the more strongly contaminated ceramic ALC, while it increases strongly at the highly pure material TAI. The decrease of the intergranular corrosion observed at ALC can be explained with the decrease of the solubility of the grain boundary phase. With the decrease of the solubility of the silicate-containing grain boundary phases, the stability of the grain boundaries of ALC approaches that of TAI. The intergranular corrosion of the high purity alumina TAI is higher than that of ALC, since TAI possesses more grain boundaries than ALC due to its smaller grain size. Since the zirconia particles at the grain boundaries of ZTA are attacked by H_2SO_4 under dissolution of Y_2O_3 followed by a cubic to monoclinic phase transformation, the resistance of ZTA against intergranular corrosion is lower up to 290°C than those of the purest alumina. In the temperature range between 340°C and 500°C ZTA was not examined.

5.3. Weight loss

The pH value of the corrosive solution, the stability and the solubility of corrosion products formed are the most important factors for the solubility of Al_2O_3 in aqueous solutions of HCl, H_2SO_4, or H_3PO_4. These factors are strongly influenced by the temperature and density of the solution and the dissociation of the acids and the corrosion products. With the increase of the temperature at a constant pressure (27 MPa), the density of the aqueous solution and the dissociation of the corrosive species are reduced. Therefore, weight losses of the alumina ceramics decrease with increasing temperature:

- HCl: An attack of the alumina grains of the materials TAI, ALC and ZTA in 0.1 mol/kg HCl only takes place at temperatures between 240°C and 290°C. The weight loss decreases thereby - except for ZTA - with increasing temperature. Solid corrosion products were not found on the samples.

  To explain the behavior of the materials in HCl, estimations of the pH-value [32] and the concentrations of the prevailing aluminum species in these solutions at 27 MPa [33] were done from literature data. Table III shows the results of these estimations for 0.1 mol/kg HCl and the applied test conditions. The amounts of the highly charged aluminum species Al^{3+} and $Al(OH)^{2+}$ are negligible in 0.1 mol/kg HCl at temperatures above 340°C, but the proportion of $Al(OH)_3$ increases strongly. Furthermore, a strong decrease of the dissociation of HCl and consequently an increase of the pH-value of 0.1 mol/kg HCl is observed in the temperature range of 300°C–350°C.

  Consequently, the temperature dependency of the weight loss of alumina ceramics and ZTA in 0.1 mol/kg HCl can be explained as follow: At 240°C, HCl is dissociated completely and the alumina solubility is high due to the high stability of Al^{3+} and $Al(OH)^{2+}$. Here, the largest weight loss of ALC and TAI was measured. If the temperature is increased to 290°C, then the dissociation of HCl is reduced already noticeably. The solubility of alumina and accordingly the weight loss of the alumina ceramics and ZTA decrease due to the increase of the temperature and the pH value, which both cause a decrease of Al^{3+} and $Al(OH)^{2+}$. With a further increase in temperature, this trend intensifies. At 340°C only a small amount of $Al(OH)^{2+}$ is still present and at temperatures above 390°C, only $Al(OH)_3$ is stable. Therefore, the solubility of Al_2O_3 in 0.1 mol/kg HCl is very small at these temperatures.

TABLE III Estimations of the pH value [32] and the content of aluminum species in 0.1 mol/kg HCl at 27 MPa

	240°C	290°C	340°C	390°C	420°C	440°C	500°C
pH (0.1 mol/kg HCl)	1.0	1.1	1.5	3.6	6.4	7.2	8.2
Al^{3+} (%)	30	—	—	—	—	—	—
$Al(OH)^{2+}$ (%)	70	60	5	—	—	—	—
$Al(OH)_2^+$ (%)	—	30	55	—	—	—	—
$Al(OH)_3$ (%)	—	10	40	100	100	100	100

- H_2SO_4: Although the dissociation of H_2SO_4 is comparable with the dissociation of HCl in the temperature range of 240°C–500°C [34], the weight losses after 50 hours of exposure in H_2SO_4 (0.7–4.5 mg/cm^2 at 240°C, 1.7–6.5 mg/cm^2 at 290°C, 7.9–8.4 mg/cm^2 at 340°C and 6–7 mg/cm^2 at 390°C) are substantially higher than those found in HCl (0.3–1.1 mg/cm^2 at 240°C, 0.1–0.5 mg/cm^2 at 290°C and <0.05 mg/cm^2 at 340–390°C). At 500°C, the behaviour of the ceramics in both acids is similar. This result can be explained with the formation of aluminum sulfate complexes such as $Al(SO)_4^+$ and $Al(SO_4)_2^-$. For lower temperatures, an increase of the solubility of gibbsite ($Al(OH)_3$) in diluted aqueous H_2SO_4 by complex formation was described by Ridley *et al.* [35] and Packter *et al.* [36].

At lower temperatures and higher acid concentrations, a different corrosion behavior of alumina ceramics was determined by Genthe and Hausner [5]. An alumina ceramic with >99.9% Al_2O_3 and 530 ppm MgO showed only a small weight loss of 0.55 mg/cm^2 after 168 hours of exposure in concentrated H_2SO_4 at 160°C, but 8.13 mg/cm^2 in concentrated HCl. Dawihl and Klingler [3] found a substantially higher weight loss of 3 mg/cm^2*d for a MgO doped, less pure alumina ceramic (99.7% Al_2O_3) in 70% H_2SO_4 at 160°C. In boiling 20% H_2SO_4, the weight loss is somewhat higher than in 20% boiling HCl. The different behavior of the aluminas in this two investigations is most likely due to the different purity of the examined materials.

The differences of the weight losses of alumina found by Genthe and Hausner [5] at 160 °C and the results in this work - in more diluted solution at temperatures between 240°C and 390°C - can be explained with a decreasing solubility of alumina in HCl with increasing temperature and a increasing solubility in H_2SO_4 with increasing temperature.

- H_3PO_4: The formation of a dense, protecting $AlPO_4$-layer prevents a high weight loss of the aluminas in H_3PO_4 in the temperature range between 240°C and 500°C. A corrosion retarding effect has the small degree of dissociation of 0.1 mol/kg H_3PO_4, which is under 5% in the examined temperature range [37]. The severe weight loss, which was found in investigations of Genthe and Hausner [5], is caused by the high solubility of the corrosion products in concentrated H_3PO_4 at 160°C.

6. Conclusions

In this work, the corrosion resistance of alumina ceramics and ZTA in aqueous acidic solutions (HCl, H_2SO_4, H_3PO_4) under hydrothermal conditions was examined systematically. The dominant corrosion mechanisms were identified as intergranular attack and dissolution of Al_2O_3.

The intensity of the grain boundary attack depends on the material purity, since impurities like SiO_2 and CaO or sintering aids like MgO have only a small solubility in Al_2O_3 and move to the grain boundaries during the sintering process where they segregate or form a grain boundary phase. Accordingly, the high purity alumina TAI generally shows the highest resistance against intergranular corrosion. ZTA is more resistant against intergranular attack than ALC due to the ZrO_2-particles at the grain boundaries.

An increase of the temperature at a constant pressure of 27 MPa causes a strong decrease of density and acid dissociation in the temperature range between 340°C and 400°C. The solubilities of oxides, the grain boundary phases and the formed corrosion products therefore decrease with increase of the temperature over approx. 360°C.

In HCl, the solubility of Al_2O_3 decreases with increasing temperature and is negligible at temperatures above 340°C, since the stability of Al^{3+} and $Al(OH)^{2+}$ decreases. Consequently, the weight loss is low above 340°C. In H_2SO_4, the solubility and the dissolution rate of Al_2O_3 and the corrosion products are high up to a temperature of 290°C and a high weight loss is found. At temperatures above 340°C, the solubility of the corrosion products decreases and a non-protecting corrosion layer is formed. Nevertheless, the weight loss is high up to a temperature of 390°C. The higher weight loss in H_2SO_4, compared with that in HCl, is probably caused by the formation of complexes such as $Al(SO_4)^+$ and $Al(SO_4)_2^-$. In H_3PO_4, a protecting $AlPO_4$-layer is formed in the temperature range between 240°C and 500°C, and the weight loss is small.

Acknowledgements

The authors would like to thank C. Friedrich, G. Franz, W. Habicht, and P. Kritzer for supporting this work.

References

1. K. ODA and T. YOSHIHO, *J. Am. Ceram. Soc.* **80** (1997) 3233.
2. S. KITAOKA, Y. YAMAGUCHI and Y. TAKAHASHI, *ibid.* **75** (1992) 3075.
3. W. DAWIHL and E. KLINGLER, *Ber. DKG* **44** (1967) 1.
4. W. GENTHE and H. HAUSNER, in "Euroceramics," edited by G. de With and R. A. Terpstra (Elsevier Applied Science, London, 1989) p. 3463.
5. *Idem., cfi/Ber. DKG* **67** (1990) 6.
6. *Idem., J. Eur. Ceram. Soc.* **9** (1992) 417.
7. M. MODELL, US Patent 4,338,199, 6.7 (1982).
8. P. KRITZER, N. BOUKIS and E. DINJUS, *Mater. Corros.* **48** (1997) 799.
9. *Idem.*, Proceedings EUROCORR'97, Trondheim, Norway, 22–25 September, 1997, Vol. II, p. 229.
10. *Idem., Corrosion* **54** (1998) 824.
11. *Idem., ibid.* **54** (1998) 689.
12. N. BOUKIS, N. CLAUSSEN, K. EBERT, R. JANSSEN and M. SCHACHT, *J. Eur. Ceram. Soc.* **17** (1997) 71.
13. N. BOUKIS and M. SCHACHT, DE-Patent 44 43 452 C2, 19.12 (1996).
14. S. K. ROY and R. L. COBLE, *J. Am. Ceram. Soc.* **51** (1968) 1.
15. R. W. GRIMES, *ibid.* **77** (1994) 378.
16. W. C. JOHNSON and D. F. STEIN, *ibid.* **58** (1975) 485.
17. R. F. COOK and A. G. SCHROTT, *ibid.* **71** (1988) 50.
18. S. BAIK and J. H. MOON, *ibid.* **74** (1991) 819.
19. K. K. SONI, A. M. THOMPSON, M. P. HARMER, D. B. WILLIAMS, J. M. CHABALA and R. LEVI-SETTI, *Appl. Phys. Lett.* **66** (1995) 2795.
20. R. BRYDSON, S. C. CHEN, F. L. RILEY, S. J. MILNE, X. PAN and M. RÜHLE, *J. Am. Ceram. Soc.* **81** (1998) 369.
21. W. SWIATNICKI, S. LARTIGUE-KORINEK and J. V. LAVAL, *Acta metall. mater.* **43** (1995) 795.
22. C. A. HANDWERKER, P. A. MORRIS and R. L. COBLE, *J. Am. Ceram. Soc.* **72** (1989) 130.
23. S. C. HANSEN and D. S. PHILLIPS, *Phil. Mag. A* **47** (1983) 209.
24. T. SAKUMA, Y. IKUHARA, Y. TAKIGAWA and P. THAVORNITI, *Mater. Sci. Eng. A* **234–236** (1997) 226.
25. Y. TAKIGAWA, Y. IKUHARA and T. SAKUMA, *Mater. Sci. For.* **243–245** (1997) 425.
26. F. WAKEI, T. NAGANO and T. IGA, *J. Am. Ceram. Soc.* **80** (1997) 2461.
27. H. YOSHIDA, K. OKADA, Y. IKUHARA and T. SAKUMA, *Phil. Mag. Lett.* **76** (1997) 9.
28. O. FLACHER, J. J. BLANDIN and K. P. PLUCKNETT, *Mater. Sci. Eng. A* **221** (1996) 102.
29. S. J. BENNISON and M. P. HARMER, in "Ceramic Transactions, Vol. 7: Sintering of Advanced Ceramics," edited by C. A. Handwerker, J. E. Blendell and W. Q. Kaysser (American Ceramic Society, Westerville, OH, 1990) p. 13.

30. S. BAIK, D. E. FOWLER, J. M. BLAKELY and R. RAJ, *J. Am. Ceram. Soc.* **68** (1985) 281.
31. S. BAIK, *ibid.* **69** (1986) C101.
32. J. D. FRANTZ and W. L. MARSHALL, *Am. J. Sci.* **284** (1984) 651.
33. V. A. POKROVSKII and H. C. HELGESON, *Am. J. Sci.* **295** (1995) 1255.
34. T. XIANG, K. P. JOHNSON, W. T. WOFFORD and E. F. GLOYNA, *Ind. Eng. Chem. Res.* **35** (1996) 4788.
35. M. K. RIDLEY, D. J. WESOLOWSKI, D. A. PALMER, P. BÉNÉZETH and R. M. KETTLER, *Environ. Sci. Technol.* **31** (1997) 1922.
36. A. PACKTER and H. S. DHILLON, *J. Chem. Soc. (A)* (1969) 2588.
37. H. C. HELGESON, *J. Phys. Chem.* **71** (1967) 3121.

Received 25 November 1998
and accepted 30 May 2000